Fission and Reaction Cross Sections in the Uranium Region with 4- to 12-MeV Protons*

GEORGE L. BATE† AND J. R. HUIZENGA
Argonne National Labroatory, Argonne, Illinois
(Received 9 October 1963)

Fission fragment angular distributions have been measured with gold surface barrier detectors for proton-induced fission of U^{233}, U^{234}, U^{235}, U^{236}, U^{238}, Np^{237}, and Pu^{239}. Absolute fission cross sections were determined for U^{233} and U^{238}. The proton projectile energy range of 4–12 MeV was obtained with the Argonne tandem Van de Graaff. Over this energy range the fission cross section of U^{233} changed by a factor exceeding a million. Total reaction cross sections were calculated for the highly fissionable U^{233} target by applying small corrections (3 to 20%) for the spallation cross sections. These reaction cross sections are compared with theoretical values deduced from surface absorption optical-model calculations with parameters of Perey and Wilkins.

I. INTRODUCTION

THE two principal methods for obtaining reaction cross sections with charged particle projectiles consist of (1) direct attenuation measurements of incident beam intensity and (2) summation of separately determined partial reaction cross sections. Method (1) is subject to inaccuracy in the heavy element mass region for the proton energy range of 4–12 MeV because experimental techniques employed have not circumvented copious Rutherford scattering from high-Z nuclei. For heavy elements such as those studied in this work, fission may be the dominant compound nucleus exit channel when the excitation energy is adequate. With sufficiently large values of Γ_f/Γ_t, the ratio of fission to total level width, the fission cross section directly gives by method (2) a first approximation to the total reaction cross section.

Little data on reaction cross sections for the heavy element region in the proton energy range of 4–12 MeV are available in the literature. Reaction cross section data for several elements up to the uranium region are given for 10-MeV protons in recent work by Wilkins and Igo.[1] In the present work, fission cross sections for U^{233} and U^{238}, typical fissionable species in the U-Pu region, have been measured as a function of proton energy. These cross sections are then used to approximate the reaction cross sections by method (2), which in turn permit further assessment of the optical-model parameters in the heavy element mass region. Anisotropy measurements have been obtained also for U^{234}, U^{235}, U^{236}, Np^{237}, and Pu^{239} in this work.

II. EXPERIMENTAL RESULTS

Proton bombardments were carried out with the Argonne tandem Van de Graaff accelerator, which provided continuously variable proton energies up to 12 MeV with a beam energy dispersion of approximately 10 keV. Fission fragments were detected with 100–200 Ω-cm gold surface barrier junction counters, which produced an electronic pulse with an amplitude proportional to the energy deposited by the fission fragment. These pulses were amplified and then sorted and recorded in a 256-channel analyzer. Details of target fabrication, scattering chamber construction, and electronics system have beeen given in previous reports.[2,3]

Differential cross section ratios for U^{233}, U^{234}, U^{235}, U^{236}, U^{238}, Np^{237}, and Pu^{239} are shown in Figs. 1 and 2, where the ratio of the count rates at 170° and 90°,

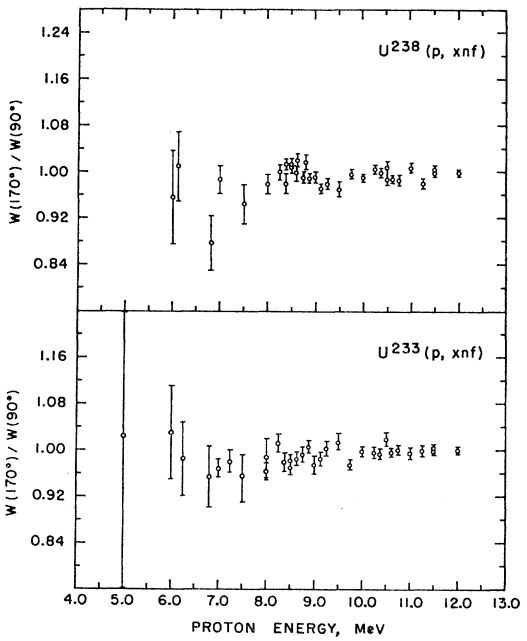

FIG. 1. Angular distributions W(170°)/W(90°) in center-of-mass coordinates for fission fragments produced by proton interaction with U^{233} (lower section) and with U^{238} (upper section). The plotted points are experimental values with statistical uncertainties.

* Based on work performed under the auspices of the U. S. Atomic Energy Commission.
† Permanent address: Department of Physics, Wheaton College, Wheaton, Illionois.
[1] B. D. Wilkins and G. Igo, Phys. Rev. **129**, 2198 (1963).
[2] G. L. Bate, R. Chaudhry, and J. R. Huizenga, Phys. Rev. **131**, 722 (1963).
[3] J. R. Huizenga, R. Chaudhry, and R. Vandenbosch, Phys. Rev. **126**, 210 (1962).

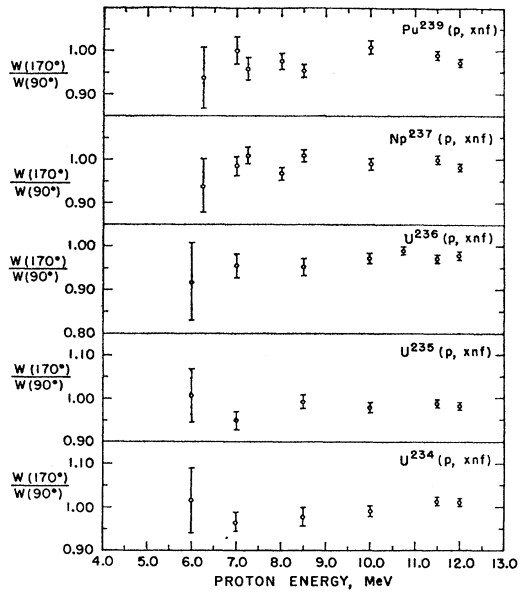

FIG. 2. Angular distributions W(170°)/W(90°) in center-of-mass coordinates for fission fragments produced by proton interaction with U^{234}, U^{235}, U^{236}, Np^{237}, and Pu^{239} shown, respectively, in the lower to upper frames.

W(170°)/W(90°), in center-of-mass coordinates, is plotted as a function of proton laboratory energy. For all nuclides the anisotropy does not exceed unity by an appreciable amount, in no case reaching the values of 1.03, 1.05, 1.09, and 1.07 (uncertainty ± 0.03 in each case) reported by Coffin and Halpern[4] for 10 MeV proton-induced fission of the respective nuclides Pu^{239}, Np^{237}, U^{235}, and U^{238}. Optical-model calculations for 10-MeV protons on heavy nuclei give a value for $\langle l^2 \rangle$ of approximately 5, and hence, the expected anisotropy is very small. Although a small anisotropy may be masked by the statistical fluctuations of the data, the angular distributions are interpreted as being essentially isotropic, and on this basis the fission cross sections for U^{233} and U^{238} are calculated.

Fission cross sections for U^{233} and U^{238} are displayed in Fig. 3 as a function of proton laboratory energy. Measurements over a wider range of energy, from 4 MeV to 12 MeV, were made with U^{233} which showed a variation in fission cross section by a factor of over 10^6, the point at 4 MeV essentially comprising an upper limit. The $U^{238}(p,xnf)$ fission cross sections may be compared with those reported by Choppin *et al.*[5] The agreement is reasonably good (within $\sim 10\%$) above 6 MeV but is poor below 6 MeV. For example, our measured upper limit of the σ_f at 4 MeV for U^{233} is a factor of 40 less than that for U^{238} determined by Choppin *et al.*[5] (Note in Fig. 3 that the σ_f of U^{233} is larger than that of U^{238} at all bombarding energies.)

The relative variation in fission cross sections for U^{233} and U^{238} as a function of energy is of interest. The small relative differences in cross section are not readily discernible in Fig. 3, but are apparent in Fig. 4 where the ratio of the fission cross sections, $\sigma_f(U^{233})/\sigma_f(U^{238})$ is plotted as a function of proton energy. In the vicinity of 7 to 8.5 MeV it is seen that the ratio of the cross sections undergoes a marked decrease, presumably due to an increase in the U^{238} fission cross section at a faster rate than the U^{233} fission cross section. Since the level width ratio Γ_f/Γ_T is larger for Np^{234} than for Np^{239}, it would be reasonable to assume that the net fission cross section for $U^{238}(p,xnf)$ appreciates with increasing proton energy faster than that for $U^{233}(p,xnf)$. In particular, the region of 7 to 8.5 MeV very likely corresponds to the onset of second chance fission in Np^{239}, the compound nucleus now having sufficient excitation energy to undergo fission after the emission of a neutron, in addition to the continuing first chance fission events. Although second chance fission for U^{233} probably sets in at approximately the same energy, the effect is not as marked because the probability for first chance fission was already large. That the change in the $\sigma_f(U^{233})/\sigma_f(U^{238})$ ratio is due primarily to the Np^{239} chain rather than the Np^{234} chain is verified by the fact

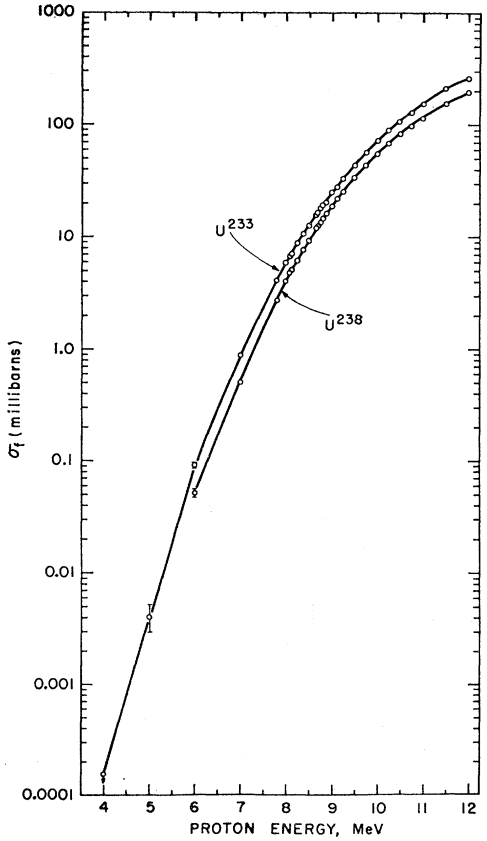

FIG. 3. Excitation functions for proton-induced fission of U^{233} (upper curve) and U^{238} (lower curve). Statistical errors are shown at lower energies where they exceed the geometrical size of the encircled plots. The arrow at 4 MeV indicates that the measured U^{233} cross section is an upper limit.

[4] C. T. Coffin and I. Halpern, Phys. Rev. **112**, 536 (1958).

that plots of the ratios of $\sigma_f(Np^{237})/\sigma_f(U^{238})$ and of $\sigma_f(Pu^{239})/\sigma_f(U^{238})$ are very similar in shape to that of Fig. 4. Since Np^{237} and Pu^{239}, like U^{233}, are more fissionable than U^{238}, the concordant trends in the ratios of the fission cross sections are consistently attributed to a controlling contribution from the Np^{239} chain.

Level width ratios Γ_n/Γ_f for U^{233} and U^{238} proton fission may be computed from the data of Fig. 4 if the dependence of Γ_f/Γ_n on mass number is known. Simultaneous equations for an assumed variation $\Gamma_n/\Gamma_f = Ce^{\lambda A}$ (C, λ undetermined constants; mass number $= A$) were investigated. It was found that values of C and λ so determined were sensitive to small changes in $\sigma_f(U^{233})/\sigma_f(U^{238})$ to such an extent that even over the small range of statistical errors, the effect on values of C and λ was marked. While the assumed dependence of Γ_n/Γ_f on A may be reasonable as a general trend,[6] its validity for two specific members of the chain, especially for excitation energies approaching fission threshold, may be open to question. Whatever the form of Γ_n/Γ_f dependence on A, it is here concluded that useful evaluation of undetermined constants must await a much more accurate determination of the cross section ratios.

Previous estimates of level width ratios[6] may be checked by comparing values of the fission cross section ratio calculated from level width ratios with the experimental value of the fission cross section ratio. It is reasonable to assume that for the relevant excitation energies, level widths for gamma and charged particle emission may be neglected so that to a good approximation, the total level width Γ_T is given by the sum of the fission and neutron emission level widths: $\Gamma_T = \Gamma_f + \Gamma_n$.

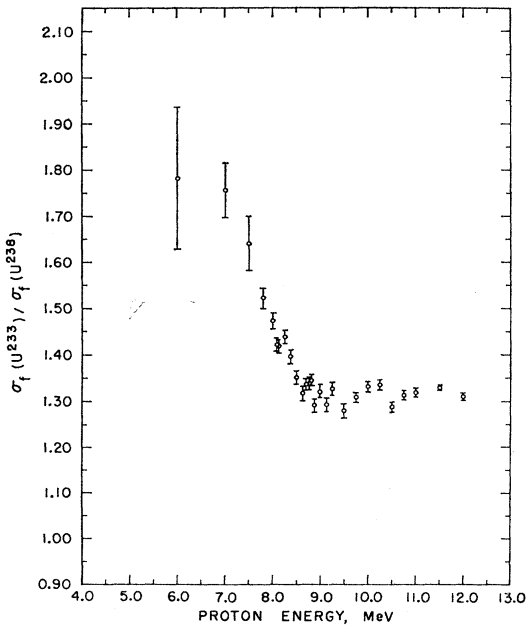

FIG. 4. Ratio of the proton fission cross sections, $\sigma_f(U^{233})/\sigma_f(U^{238})$, as a function of laboratory proton energy.

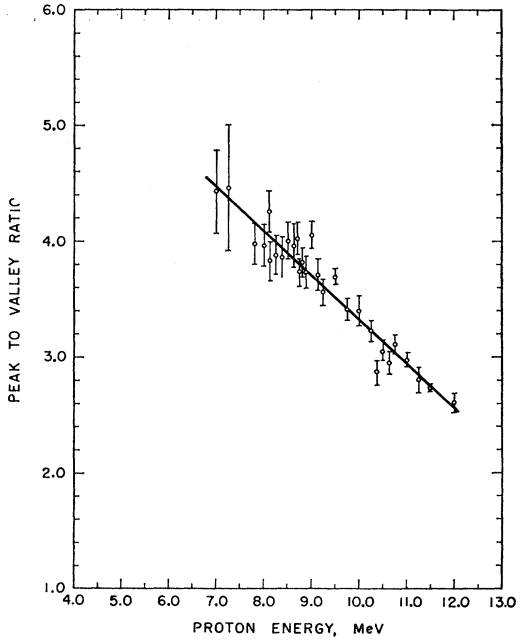

FIG. 5. U^{238} fission peak-to-valley ratios as a function of proton laboratory energy.

Then for two-chance fission events following proton excitation of a target nuclide of atomic number Z and mass number A, the reaction cross section σ_R may be written as

$$\sigma_R(Z,A)=\sigma_f(Z,A)\{(\Gamma_f/\Gamma_T)_{Z+1,A+1}+(\Gamma_f/\Gamma_T)_{Z+1,A}[1-(\Gamma_f/\Gamma_T)_{Z+1,A+1}]\}^{-1}. \quad (1)$$

Assuming the reaction cross sections for proton excitation of U^{233} and U^{238} to be negligibly different, the ratio of the fission cross sections $\sigma_f(U^{233})/\sigma_f(U^{238})$ may be calculated from Eq. (1) as a function of only the level width ratios. Using the values[6] $(\Gamma_f/\Gamma_T)_{Np^{234}}=0.80$, $(\Gamma_f/\Gamma_T)_{Np^{238}}=0.85$, $(\Gamma_f/\Gamma_T)_{Np^{239}}=0.42$, and $(\Gamma_f/\Gamma_T)_{Np^{238}}=0.53$, the ratio $\sigma_f(U^{233})/\sigma_f(U^{238})$ calculated in this manner from Eq. (1) is 1.3, which may be compared with the average of 1.3 over the energy range of 9–12 MeV in Fig. 4. Over the 9–12 MeV energy range it is reasonable to expect the fission cross section to be comprised of first and second chance fission events. Below 7 MeV the value of the fission cross section ratio calculated with Eq. (1) modified for single chance fission is 1.9, which is in approximate agreement with the experimental value in Fig. 4 in view of the considerable statistical uncertainty at these low energies.

Additional data on U^{238} fission are given in the form of peak-to-valley ratios (computed from high-energy peak) shown in Fig. 5 as a function of proton laboratory energy. If the changes in peak-to-valley ratio are attributed to changes in relative proportions of asymmetric and symmetric modes of fission, then it is seen from the figure that the frequency of the symmetric

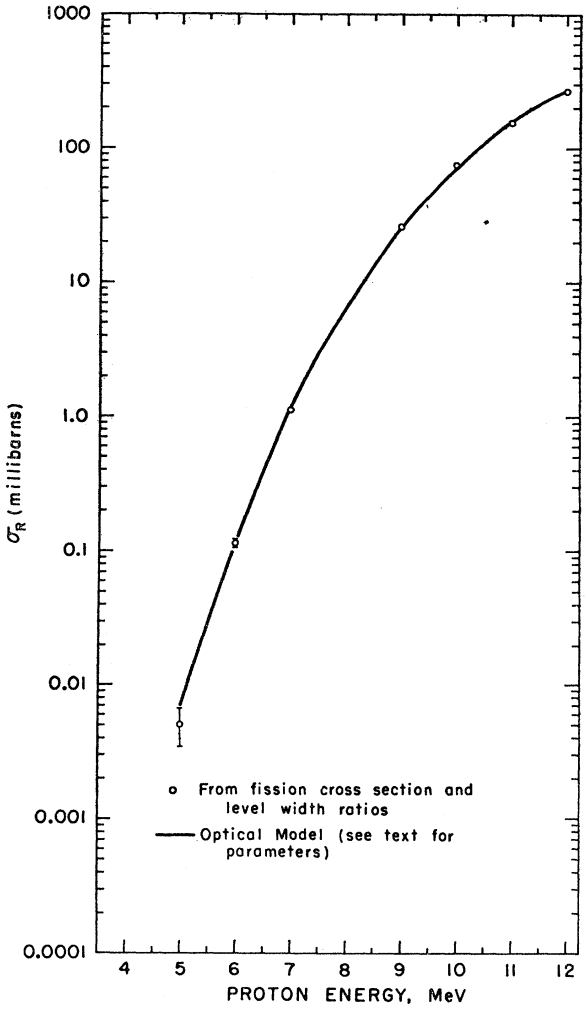

FIG. 6. Total reaction cross sections obtained from level width ratios and fission cross sections. The solid curve represents theoretical values based on optical-model calculations using parameters after Perey (Ref. 9).

mode increases in an essentially linear manner with proton energy over this energy range. These peak-to-valley ratios were determined for a detector 170° from the forward beam direction, and may be compared with the values of Choppin *et al.*[5] for the 90° detector position. The two sets of data differ in at least three respects: (1) The values in Fig. 5 are higher by nearly a factor of two; (2) the slope in Fig. 5 is more uniformly linear than that shown in the Florida State work; (3) possible discontinuities in the data of Fig. 5 are only suggested (in the vicinity of 8.3 and 10.6 MeV) and perhaps because of the statistical fluctuations, do not appear as clearly defined as the discontinuities in peak-to-valley ratios obtained by Choppin *et al.* as a function of proton energy. The reasons for these differences evidenced from interlaboratory comparison are not readily discernible.

The measurement of fission cross sections with a proton beam of sharply defined energy may also provide an indirect probe of nuclear level density and distribution. The statistical fluctuation of nuclear cross sections has been treated by Ericson,[7] on the basis of statistical assumptions that nuclear levels are spaced randomly and that level widths also exhibit random distribution. In the case of fission, the compound nucleus formed by proton interaction with the target nucleus populates excited states above the saddle; consequently, possible fluctuations in fission cross sections reflect the nature of the distribution of excited states above the saddle deformation. In order to detect possible fine-structure resonance effects, a U^{238} target with a thickness of less than 5-keV proton degradation was bombarded with 10-MeV protons, and several fission cross sections were measured for proton energy increments of 10 keV. The spread in proton energy throughout the target is of the order of the energy increment. The results are given in Table I. When allowance is made for the broad nonresonant energy dependence of these cross sections, no appreciable short-period fluctuations are evident beyond the uncertainties from counting statistics. For the approximately 10 MeV of excitation energy available at the saddle point, this result is consistent with the participation of many final states above the saddle in the case of the dominant first chance fission events. The effects of possible fine structure for second chance fission following neutron emission are annuled by the distribution in kinetic energy of the emitted neutron. This test over a very limited energy range is not amenable to broad generalization. In particular, resonance fluctuations in fission cross sections may be characteristic of low-energy excitations where the level densities are greatly reduced near the fission threshold.

III. TOTAL REACTION CROSS SECTIONS

In the absence of further direct experimental measurements, the level width ratios which have been shown compatible with the present fission cross section data, may now be taken for approximation of the reaction

TABLE I. Fission fragment angular distributions and cross sections for a 5-keV thick U^{238} target tabulated against proton laboratory energy in increments of 0.01 MeV. The energy resolution of the beam is approximately equal to the energy increment.

Energy (MeV)	W(170°)/W(90°)	σ_f(mb)
10.00	1.000±0.006	55.0±0.2
9.99	1.008±0.006	54.5±0.2
9.98	1.001±0.006	53.9±0.2
9.97	1.009±0.009	53.8±0.2
9.96	0.996±0.007	53.1±0.2

[5] G. R. Choppin, J. R. Meriwether, and J. D. Fox, Phys. Rev. **131**, 2149 (1963).

[6] R. Vandenbosch and J. R. Huizenga, in *Proceedings of the Second United Nations International Conference on the Peaceful Uses of Atomic Energy, Geneva, 1958* (United Nations, New York, 1958), Vol. 15, p. 284.

[7] T. Ericson, Advan. Phys. **9**, 425 (1950).

cross section. Using Eq. (1), the reaction cross section for U^{233} is found by multiplying the fission cross section by the reciprocal of the quantity appearing in braces on the right. Substitution of the level width ratios gives the value of this factor as 1.03 for the 9 to 12 MeV region corresponding to first and second chance fission, and gives the value of 1.20 for first chance fission events only below 7 MeV. The total reaction cross sections determined in this manner from the fission cross sections of U^{233} are plotted in Fig. 6.

The solid curve shown in Fig. 6 represents the theoretical reaction cross section as a function of energy, determined by optical model calculations with the Abacus II program.[8] The central potential for the optical model used consists of a real part

$$V_{\mathrm{Re}}(r)=-V_s[1+e^{(r-R_c)/a}]^{-1}, \qquad (2)$$

and an imagniary part

$$V_{\mathrm{Im}}(r)=-4bW_D d/dr[1+e^{(r-R_c)/b}]^{-1}. \qquad (3)$$

The imaginary term includes surface absorption only and is based on the radial derivative of the usual Saxon form factor. V_s, a, W_D, and b are amplitude and exponential parameters for the central potential. The Coulomb potential used in the optical model is that produced by a uniform spherical charge distribution of radius R_c. The spin-orbit potential is of the Thomas form with real term only, amplitude V_{so}.

The choice of optical-model parameters for the theoretical evaluation incorporated in Fig. 6 is based, in the absence of elastic scattering data in the uranium region, on the results of a study by Perey,[9] who has carried out a form of least-squares fit to proton elastic scattering and reaction cross section data for elements ranging from aluminum to gold. Perey's analysis has led to a "best choice" of parameters as a function of mass number and energy, and their incorporation here provides a partial test of their validity in the heavy element mass region of uranium. Following Perey, the values of the optical-model parameters are therefore taken as follows: $R_c=1.25A^{1/3}$ F (the Coulomb radius R_c is also used as the value of the well radius), $a=0.65$ F, $W_D=3.5A^{1/3}$ MeV, and $V_{so}=7.5$ MeV. Values for the amplitude of the real central potential function are evaluated from Perey's semiempirical expression

$$V_s=53.3-0.55E+0.4Z/A^{1/3}+27(N-Z)/A\,, \qquad (4)$$

where E is the proton energy in MeV, and Z, N, and A are the usual proton, neutron, and mass numbers, respectively.

According to Perey, the surface diffuseness parameter b taken as 0.47 F gave best fits for most elements; but evidence was presented which showed that for the heavier elements (up to gold), better fits to the elastic scattering data were obtained for b increased to 0.65 F. Since the elastic scattering data generally involve more stringent requirements on the optical-model parameters for good fits than do reaction cross sections, the evidence of Perey was accepted as a valid basis for variation of b to obtain closest approximation to the reaction cross sections while providing simultaneously optimum probability of best fit for scattering requirements. The value of b found to give the fit shown in Fig. 6 is 0.59 F.

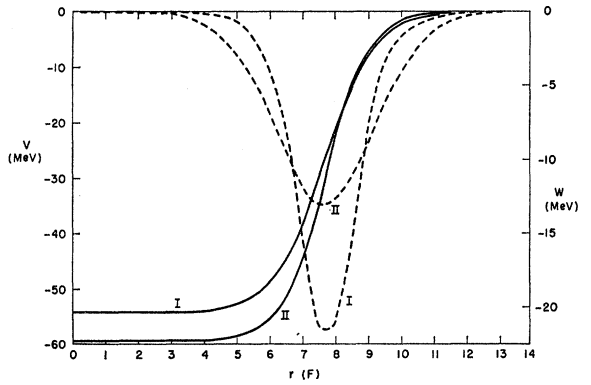

FIG. 7. Real (———) and imaginary (– – – –) optical-model potential functions with parameters after Perey (I) and suggested by Wilkins (II) as a function of nuclear distance measured in fermis.

If the small mass dependence of σ_R is neglected, the theoretical values of σ_R in Fig. 6 obtained by optical-model calculations for U^{233} may be compared with those of Choppin *et al.*[5] obtained for U^{238} also by use of the optical model. The theoretical reaction cross sections given for U^{238} exceed those in Fig. 6 by factors varying from about 3 to 5. These larger reaction cross sections obtained for U^{238} by Choppin *et al.* are due to their choice of a very large radius parameter for the optical-model calculations.

That the optical-model parameters are not unique, is demonstrated by an equally good fit to the data of Fig. 6 obtained with a different set of parameters. The values of these parameters were suggested by Wilkins on the basis of an extrapolation from his fits for proton reaction cross sections at 10 MeV[10] and employ a Gaussian form factor for surface absorption, without spin-orbit coupling: $r_0=1.24$F (well radius parameter), $a=0.75$F, $b=2.20$F, and $W_D=13.0$ MeV; $V_s=54.3$ MeV at 10 MeV, with an energy dependence of $-0.55E$ adapted from Perey. The reaction cross sections obtained with this set of parameters essentially duplicates the theoretical curve shown in Fig. 6. The potentials for the two sets of parameters are displayed in Fig. 7 as a function of the radial distance from the center of the nucleus. While set I curves (after Perey) exhibit greater depth than set II curves (Wilkins), the greater spatial extent of the latter may partially offset their lack of

[8] The authors are indebted to E. H. Auerbach and C. E. Porter of Brookhaven National Laboratory for the revised version Abacus II optical-model program.

[9] F. G. Perey, Phys. Rev. **131**, 745 (1963).

[10] B. D. Wilkins, University of California Radiation Laboratory Report UCRL-10783, 1963 (unpublished).

potential depth; but a regorous explanation of a common reaction cross section for the two sets of curves is hindered by the present limited understanding of the physical significance of the optical model parameters.

The different sets of values of optical model parameters obtained by Perey and by Wilkins apparently originate in the basically different search programs used by each investigator to obtain best fits to elastic scattering and reaction cross section data. Since both sets of parameters give convergent fits for the reaction cross section data of this work, a more stringent test must await the availability of experimental elastic scattering angular distributions in the uranium region.

ACKNOWLEDGMENTS

The authors are indebted to T. H. Braid for the use of his 18-in. scattering chamber. Our further appreciation is expressed to B. D. Wilkins for helpful discussions on the optical model and to J. K. Munro for technical assistance.

PHYSICAL REVIEW VOLUME 133, NUMBER 6B 23 MARCH 1964

Inelastic Scattering of Neutrons by Tritons*

J. L. GAMMEL† AND A. D. MACKELLAR‡
Los Alamos Scientific Laboratory, University of Catifornia, Los Alamos, New Mexico
(Received 5 November 1963)

Assuming that the range of nuclear forces is small compared to the size of the triton and the wavelength of the incoming neutron ("zero-range" approximation), we derive a connection between the cross sections for elastic and inelastic n–t scattering by calculating the ratio of the first Born approximation for inelastic to that for elastic scattering. A calculation of the inelastic scattering cross section is made for an incoming neutron energy of 14 MeV. Since experimental elastic angular distributions are not available, we use values calculated by Bransden and Robertson for p–He^3 assuming Serber interaction. Inelastic angular distributions are calculated for the ejected deuteron, the ejected neutron, and the scattered neutron. Integrating over the distribution of the ejected deuteron, we obtain a value for the total n–t inelastic cross section of 343 mb. We realize that the calculations are very crude, but hope that the work will be helpful in planning future experiments.

I. TRITIUM WAVE FUNCTIONS

IN this paper the triton will be treated as a deuteron-neutron bound pair. The ground-state wave function of tritium may be written as the product of a spatial part symmetrical in all three coordinates 123 times an antisymmetrical spin function

$$\psi=\varphi(123)\chi_a{}^m. \tag{1}$$

Since T is a spin-$\frac{1}{2}$ particle, the spin functions are

$$\chi_a{}^{1/2}=\frac{1}{\sqrt{2}}(\alpha_1\beta_2-\beta_1\alpha_2)\alpha_3 \tag{2}$$

and

$$\chi_a{}^{-1/2}=\frac{1}{\sqrt{2}}(\alpha_1\beta_2-\beta_1\alpha_2)\beta_3. \tag{3}$$

The space function after elastic scattering is

$$\Phi=\frac{\varphi(\mathbf{r})f(\mathbf{q})+\varphi(\mathbf{q}+\frac{1}{2}\mathbf{r})f(-(q/2)+\frac{3}{4}\mathbf{r})}{(3.344)^{1/2}}, \tag{4}$$

where $\varphi(\mathbf{r})$ is a function of the deuteron coordinates and $f(q)$ is a function of the relative coordinates of the triton. The factor $(3.344)^{1/2}$ is obtained by normalizing the integral

$$\int|\Phi|^2d\tau,$$

using

$$\varphi(r)=e^{-\alpha r}/r, \quad \alpha=0.23182F^{-1} \tag{5}$$

$$f(q)=e^{-\beta q}/q, \quad \beta=0.44743F^{-1} \tag{6}$$

and the triton is made up of neutrons at r_1 and r_2 and a proton at r_3. It is bombarded by a neutron at r_4. The following coordinates are used:

$$\mathbf{r}=\mathbf{r}_2-\mathbf{r}_3, \tag{7}$$

$$\mathbf{q}=\mathbf{r}_1-\tfrac{1}{2}(\mathbf{r}_2+\mathbf{r}_3), \tag{8}$$

$$\mathbf{Q}=\mathbf{r}_4-\tfrac{1}{3}(\mathbf{r}_1+\mathbf{r}_2+\mathbf{r}_3), \tag{9}$$

$$\mathbf{s}=\tfrac{1}{4}(\mathbf{r}_1+\mathbf{r}_2+\mathbf{r}_3+\mathbf{r}_4). \tag{10}$$

With one of its neutrons excited, the triton could either have spin $\frac{3}{2}$ or $\frac{1}{2}$.

The $S=\frac{3}{2}$ Case

$$\psi=\varphi(\mathbf{r})f_{k',q}(\mathbf{q})\chi_{3/2}{}^m - \varphi(\mathbf{q}+\tfrac{1}{2}\mathbf{r})f_{k',q}\left(-\tfrac{1}{2}\mathbf{q}+\frac{3}{r}\mathbf{r}\right)\Gamma_{3/2}{}^m, \tag{11}$$

---

* This work done under the auspices of the U. S. Atomic Energy Commission.

† Present address: Texas A & M University, College Station, Texas.

‡ Present address: Oak Ridge National Laboratory, Oak Ridge, Tennessee.